



U.S. Army Research Institute of Environmental Medicine

Natick, Massachusetts

TECHNICAL REPORT NO. T20-06
DATE April 2020

INDIVIDUALIZED AVATARS WITH COMPLETE ANATOMY: REPOSITIONING OF
SUPERFICIAL ANATOMY

Approved for Public Release; Distribution is Unlimited

United States Army
Medical Research & Development Command

DISCLAIMER

The opinions or assertions contained herein are the private views of the author(s) and are not to be construed as official or reflecting the views of the Army or the Department of Defense. The investigators have adhered to the policies for protection of human subjects as prescribed in 32 CFR Part 219, Department of Defense Instruction 3216.02 (Protection of Human Subjects and Adherence to Ethical Standards in DoD-Supported Research) and Army Regulation 70-25.

USARIEM TECHNICAL REPORT T20-06

**INDIVIDUALIZED AVATARS WITH COMPLETE ANATOMY: REPOSITIONING OF
SUPERFICIAL ANATOMY**

Zhiqing Cheng¹
Jingwen Hu²
James Yang³
Diana P. Sanford
Reed W. Hoyt
Gary P. Zientara

Biophysics and Biomedical Modeling Division
U.S. Army Research Institute of Environmental Medicine

¹Innovision LLC, Dayton, OH 45459

²Transportation Research Institute, University of Michigan, Ann Arbor, MI 48109

³Department of Mechanical Engineering, Texas Tech University, Lubbock, TX 79409

April 2020

U.S. Army Research Institute of Environmental Medicine
Natick, MA 01760-5007

REPORT DOCUMENTATION PAGE

*Form Approved
OMB No. 0704-0188*

The public reporting burden for this collection of information is estimated to average 1 hour per response, including the time for reviewing instructions, searching existing data sources, gathering and maintaining the data needed, and completing and reviewing the collection of information. Send comments regarding this burden estimate or any other aspect of this collection of information, including suggestions for reducing the burden, to Department of Defense, Washington Headquarters Services, Directorate for Information Operations and Reports (0704-0188), 1215 Jefferson Davis Highway, Suite 1204, Arlington, VA 22202-4302. Respondents should be aware that notwithstanding any other provision of law, no person shall be subject to any penalty for failing to comply with a collection of information if it does not display a currently valid OMB control number.

PLEASE DO NOT RETURN YOUR FORM TO THE ABOVE ADDRESS.

1. REPORT DATE (DD-MM-YYYY)		2. REPORT TYPE		3. DATES COVERED (From - To)	
4. TITLE AND SUBTITLE				5a. CONTRACT NUMBER	
				5b. GRANT NUMBER	
				5c. PROGRAM ELEMENT NUMBER	
6. AUTHOR(S)				5d. PROJECT NUMBER	
				5e. TASK NUMBER	
				5f. WORK UNIT NUMBER	
7. PERFORMING ORGANIZATION NAME(S) AND ADDRESS(ES)				8. PERFORMING ORGANIZATION REPORT NUMBER	
9. SPONSORING/MONITORING AGENCY NAME(S) AND ADDRESS(ES)				10. SPONSOR/MONITOR'S ACRONYM(S)	
				11. SPONSOR/MONITOR'S REPORT NUMBER(S)	
12. DISTRIBUTION/AVAILABILITY STATEMENT					
13. SUPPLEMENTARY NOTES					
14. ABSTRACT					
15. SUBJECT TERMS					
16. SECURITY CLASSIFICATION OF:			17. LIMITATION OF ABSTRACT	18. NUMBER OF PAGES	19a. NAME OF RESPONSIBLE PERSON
a. REPORT	b. ABSTRACT	c. THIS PAGE			19b. TELEPHONE NUMBER (Include area code)

TABLE OF CONTENTS

<u>Section</u>	<u>Page</u>
List of Figures.....	iv
Acknowledgments	v
Executive Summary	1
Introduction	2
Methods	4
Avatar data structure analysis and conversion.....	4
Skeleton model construction and posing	6
Template skeleton model construction.....	6
Scaling	9
Posing and motion	9
Pose mapping.....	10
Repositioning methodology development.....	11
Re-segmentation	12
Joint center determination.....	14
Mesh morphing	14
Skinning and morphing	16
Software system development.....	18
Results	18
Discussion	20
Conclusions.....	21
References.....	22

LIST OF FIGURES

<u>Figure</u>		<u>Page</u>
1	FE representation for four issue groups for IAVCA model #010244.	5
2	Display of four individual IAVCA models after conversion to Keyword format.	5
3	Two OpenSim skeleton-musculature models.	7
4	The integrated model being used as the template skeleton for IAVCA models.	8
5	Posing with OpenSim skeleton model.	10
6	Framework for IAVCA model repositioning.	11
7	IAVCA body re-segmentation. To reposition a model into different poses, we re-segmented it into 53 new parts.	13
8	Re-segmentation automatically applied to all four IAVCA models. The colors represent labels of selected anatomy identified from re-segmentation.	14
9	A simplified example to demonstrate the robustness of the combined linear blend skinning and radial basis function (LBS+RBF) repositioning method. Blue transitional elements represent those undergoing affine transformations to bend the joint. Red elements are stationary and green elements are those that undergo translation. Yellow and light blue represent two bone segments on either side of the joint. The bending results are shown with (bottom) and without (top) the bone segments.	17
10	Overall architecture of software system.	18
11	Results of case studies.	19

ACKNOWLEDGMENTS

The authors acknowledge the kind assistance of U.S. Army Natick Soldier Research, Development and Engineering Center (NSRDEC) Anthropometry Team Leader, Steven P. Paquette, and Team member Dr. Peng Li, who originally provided us with the body surface scan mesh data from which the avatars used as examples here are constructed. Also, we acknowledge financial support from the US Defense Health Agency Small Business Innovation Research Program DHA17-003, and the US Army Military Operational Medicine Research Program.

EXECUTIVE SUMMARY

This study investigated methods for rapidly repositioning the 3D finite element (FE) representations of Individualized Avatar with Complete Anatomy (IAVCA) recently developed. Repositioning posed three distinct challenges: (1) each individualized avatar has a unique surface and FE structure; (2) user expectation is for rapid execution; and (3) the repositioning of avatar superficial anatomy is expected to be accompanied by the repositioning of internal organs, musculature and skeleton during natural human movement.

This study is focused on developing a method to reposition IAVCA, ignoring the effects of gravity or applied forces on repositioned organs. Herein, we developed a systematic approach for repositioning of the superficial anatomy with nominal concomitant repositioning of internal anatomy. The steps of our approach include: (1) Conversion of the data structures to a standard form; (2) template skeleton model construction, scaling, posing and pose mapping; and (3) Model re-segmentation, joint center determination and mesh morphing. Initially, a skeleton model is created using an open-source biomechanical tool, OpenSim, to ensure the biofidelity of posing. Our approach then employs an innovative morphing method that combines radial basis functions-based mesh morphing with linear blend skinning to treat excessive soft tissue deformations due to large joint motion. A software system was developed to implement our approach. Lastly, case studies were performed to test the approach by repositioning four avatars from standing to walking, running, sitting and squatting, respectively. Case study results show that avatars can be rapidly repositioned with natural shaping of superficial anatomy using this approach.

INTRODUCTION

A recent advance in digital human modeling is the method developed by Zientara and Hoyt (1) that constructs an individualized avatar with complete anatomy (IAVCA). The IAVCA is constructed by combining a 3D body surface scan mesh and a finite element (FE) segmented, anatomically-labeled model of standard gender-specific anatomy. Their scheme uses affine transformations of a standard anatomy FE mesh (consisting of irregular tetrahedral elements) to fit within a 3D body surface scan mesh (composed of triangular faces). The computed result is a digital human avatar whose anatomy (bones, soft tissues and internal organs) is a first approximation of the individual's anatomy, residing in a body shaped and sized as depicted in the individual's surface scan.

The IAVCA models have a wide range of applications from training and education to virtual patient simulations and surgical planning, to name a few. Most of these applications require the avatar(s) to be clothed and moved through different poses and positions. Therefore, there is a clear need to develop effective methods for repositioning or articulating the model for singular position changes or for coupling sequential and simultaneous changes that can form an animation.

In injury biomechanical modeling, several studies have investigated repositioning techniques for singular FE models of the human body. Vezin et al. (2) reported that the HUMOS2 model has been equipped with posture change capability. They described two methods for repositioning the model. In the first approach, a database of pre-calculated FE model positions was used and the intermediate positions were obtained by linear interpolations between nearby positions. On the other hand, their second approach was based on interactive real-time calculations. Jani et al. (3) reported repositioning of a human body FE model using FE simulations. They have further investigated: (a) the time required for repositioning; (b) control over the bone kinematics followed; (c) anatomical correctness of the repositioned model with respect to the final bone position; and (d) the level of user intervention needed. In addition Jani et al. (4) described a methodology to generate anatomically correct postures of existing human body FE models while maintaining their mesh quality. This method is based on computer graphics techniques and permits control over the kinematics followed by the bones.

In creating whole body complete anatomy human biomedical models, computer scientists usually begin with a high resolution set of whole body medical images which are then meticulously segmented using some combination of semi-automatic and manual methods. 3DSlicer (5, 6) and ITK-SNAP (7) are two examples of such software.

Important notable examples of whole body models include the virtual family/population (ViP) models created by the IT'IS Foundation (8-10). These ViP models provide the 3D mesh of males and females of different ages, with complete anatomy of each, and in a range of moderate and high spatial resolutions. Zurich MedTech AG has developed software to reposition ViP models (11). In addition, Gosselin et al. developed repositioning functionality for the ViP models in order to parameterize their posture (9). Two approaches were developed: (a) a volume-preserving, skeleton and influence

region-based approach that allows real-time posing derived from computer graphics methods (12); and (b) a physical simulation-based approach, motivated by movement mechanics.

In addition to the animation of the ViP models, various human modeling tools and game engines are available for repositioning and animating an avatar or human model. There are examples for applications using surface mesh models, 3D FE mesh models and volumetric data (i.e. voxelized data as acquired from medical imaging). The following list represents a state-of-the-art tools list that are commonly used to reposition the different types of models.

- (1) For surface mesh models: Blender (13), 3dsMax (14), Maya (15) and Poser (11). These tools are mainly used for deforming a human shape model (i.e. a 3D surface without internal anatomy) to the desired pose and animating a model into a sequence of poses. Part blending is usually used to fuse the surface deformation in the joint region.
- (2) For skeleton and musculature models: OpenSim (16) is an open source tool for modeling human bone structure and muscles and is used for posing, kinematics and dynamics. The AnyBody software (17) is used for simulating muscle forces and joint contact forces and movements.
- (3) For biomechanical models: Total HUMAN Model for Safety (THUMS) (18), the Global Human Body Models Consortium (GHBMCC) and the Position and Personalize Advanced Human Body Models for Injury Prediction (PIPER) (19) were all developed to specifically study injuries.
- (4) For 3D human models with complete internal anatomy: The Sim4Life (11) platform provides a tool for repositioning the ViP models represented as FE meshes.
- (5) For volumetric images: Bender (20) is an open source toolkit that designed for repositioning of voxelized image data.
- (6) For dynamic shape models: SCAPE (21), Human Shapes (22-26) and a Skinned Multi-Person Linear Model (SMPL) (27) are the most commonly used tools. SCAPE (21) is a computer vision based, data driven human shape modeling tool. It uses computer vision and machine learning to create 3D avatars from ordinary 2D imagery. Human Shapes (22-26) are statistical body shape models for standing and sitting poses provided by the University of Michigan Transportation Research Institute (UMTRI). Lastly, SMPL (27), is a realistic learned model of human body shape and pose that is compatible with existing rendering engines and allows for animator control.

Repositioning of the IAVCA models poses three technical challenges that, when combined, exceed the demands of the aforementioned state-of-the-art software. Repositioning of the IAVCA models must: (1) Apply to all models, regardless of gender, size and shape, since the IAVCA models are individualized; (2) Process commands

rapidly to ensure the computational time remains within a practical limit. This is necessary as future applications may potentially need to perform simultaneous and/or sequential movements of anatomy to simulate dynamic behavior; and (3) Track movement of detailed internal anatomy in the body and to create natural poses and motion based on human biomechanics.

Facing these combined challenges, existing methods, algorithms, software programs and tools prove inadequate. Therefore, we developed a systematic approach to accomplish IAVCA repositioning that includes the following steps: (1) IAVCA data structure analysis and conversion; (2) template skeleton model construction, scaling, posing and pose mapping; and (3) model re-segmentation, joint center determination and mesh morphing. The details of this methodology and repositioning case studies are described herein.

METHODS

Avatar data structure analysis and conversion

The tetrahedral finite elements (FE) of IAVCA models are the result of morphing a model of standard human anatomy generated by the Computational Geometry Algorithms Library (CGAL) 3D mesher (28) using iso2mesh (29) front-end (1). The low-resolution (5 mm) male avatars consist of 76 anatomy labels (i.e. bone, soft tissue, fat), 869,993 tetrahedral elements and 160,038 nodes with a mean edge length of 9.2 mm. The node-to-node correspondence exists among all avatars since they were morphed from the same standard anatomy FE model. As such, the difference among the avatars depends only on the difference among their node positions. We exploit this unique feature of the original IAVCA models for repositioning.

We utilize MATLAB[®] software (MathWorks Inc.; Natick MA) for our computations. To facilitate the repositioning method development, the original IAVCA data structure was converted into (a) MATLAB[®] structure data format, which was used for the IAVCA model display in MATLAB[®] and (b) Keyword format, which is a conventional file format for FE models. The MATLAB[®] structure data format has the following constituents:

- da_tg
 - da_tg(i).eln: indices of elements for i -th tissue group
 - da_tg(i).elm: indices of nodes for each element in i -th tissue group
- da_el
 - da_el(i).tgn: index of tissue group number for i -th element
 - da_el(i).tet: indices of four node numbers for i -th element
- da_nd
 - da_nd(i).eln: index of element number for i -th node
 - da_nd(i).xyz: x - y - z of i -th node

Utilizing the MATLAB structure data described above, the IAVCA tissue groups can be displayed and a few example tissues are shown in Figure 1.

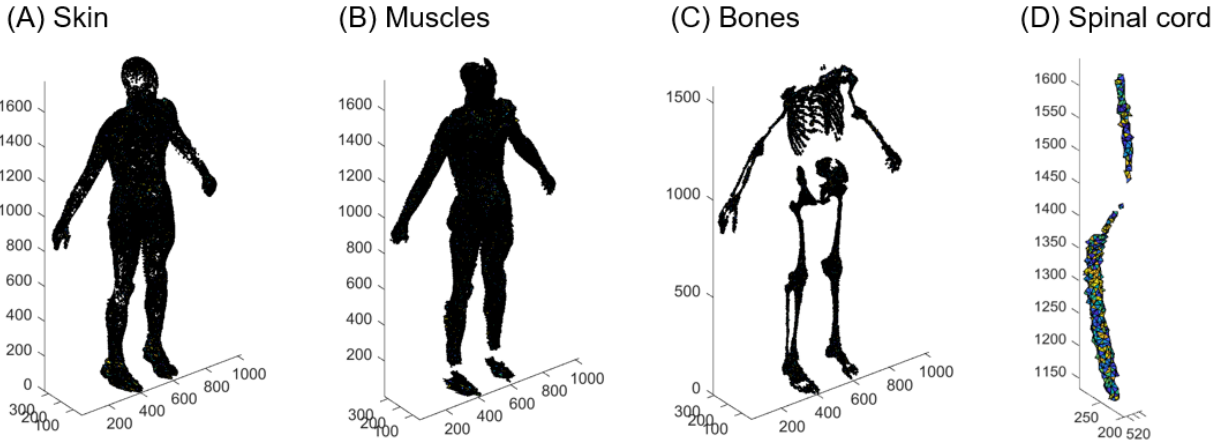


Figure 1. FE representation for four tissue groups for IAVCA model #010244.

Based on the analysis of the data structure and display of the tissue groups, several observations can be made: (1) Tissue groups are connected via shared or common nodes; (2) For each tissue group, elements can be disconnected and located in different regions of the body; (3) Mesh quality varies among tissue groups; and (4) Human articulated motion is defined by the skeleton and in terms of segment rotation. However, a segment may include elements/nodes from several tissue groups.

Alternatively, the Keyword format for an IAVCA model is composed of the following: (1) Parts.k; (2) Elements.k; and (3) Nodes for each individual model. After conversion into the Keyword format, the models can be displayed or edited with FE pre-processors, such as LS-PrePost (30) or HyperMesh (31), as shown in Figure 2.

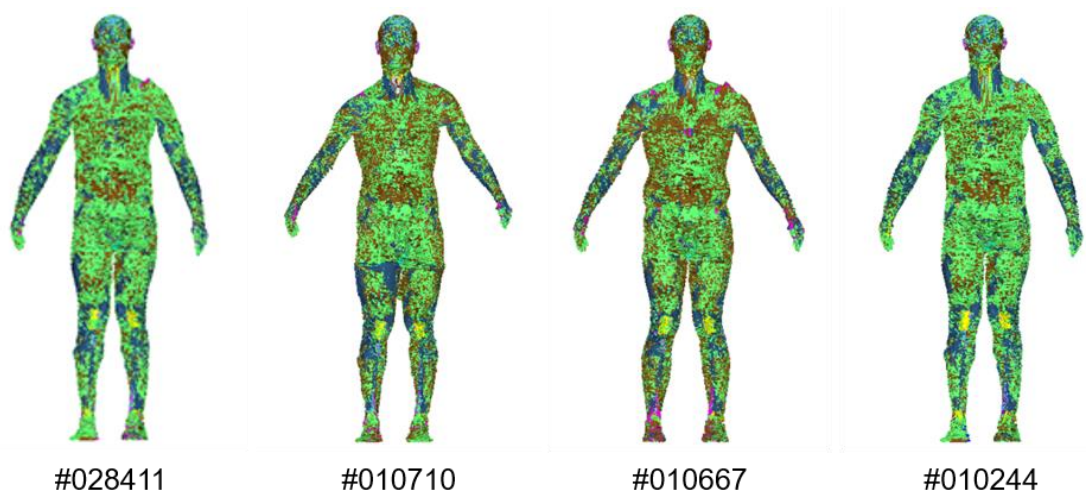


Figure 2. Display of four individual IAVCA models after conversion to Keyword format.

Skeleton model construction and posing

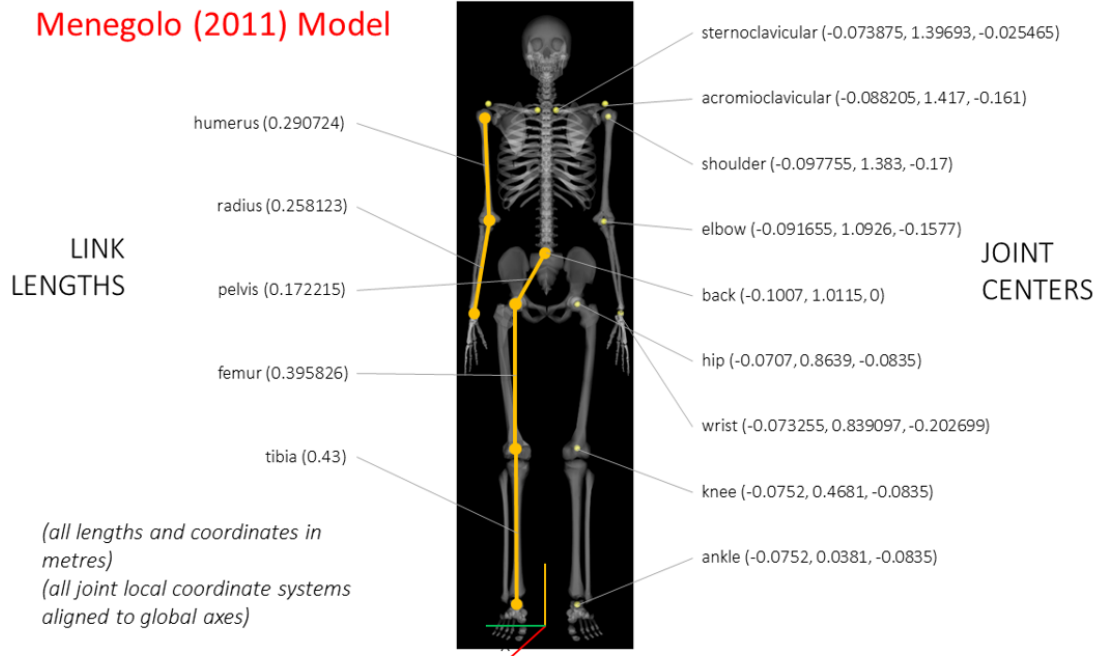
While each IAVCA model has complete anatomy, the bone structure in the model is not connected with the joints due to the low resolution. Therefore, the entire body cannot be articulated in its original FE form. To reposition an IAVCA model, a surrogate skeleton with joints needs to be established and imbedded into the model, so that it can be articulated into a desired pose or animated with the prescribed motion. The repositioning of the internal organs considering the effects of gravity and expansion or contraction of interior space in the abdomen or thoracic cavity due to changing body position is important, but beyond the scope of the present study.

Template skeleton model construction

The human pose and motion are defined and controlled by its skeleton. To ensure biofidelity and realism of the poses and dynamic motion to be created for IAVCA models, we chose to use OpenSim (16, 32) as the platform for creation and simulation of the surrogate or template skeleton model. OpenSim is a biomechanics-based, open-source tool for human static posing, kinematics and dynamics.

Through a literature review of the state-of-the-art in relevant modeling, two OpenSim skeleton-musculature models were identified. The first is the Upper Lower Body (ULB) model, which combines the lower limb model developed by Delp et al. (16) with the upper limb model developed by Holzbaaur et al (33) to create a nearly full body model without the degrees of freedom for the neck and lumbar spine (Figure 3a). A second skeleton-musculature model is the Full Body Lumbar Spine (FBLS) model (34), which was created by combining three previously developed OpenSim models (35-37). It has a fully actuated lumbar spine and a rigid but mobile torso consisting of thoracic and cervical spines, ribcage and skull. It has crudely articulated upper limbs and separate geometries for each vertebral element. The joint centers of this model are shown in Figure 3b.

(A) ULB model joint centers and bone length



(B) FBLS model joint centers

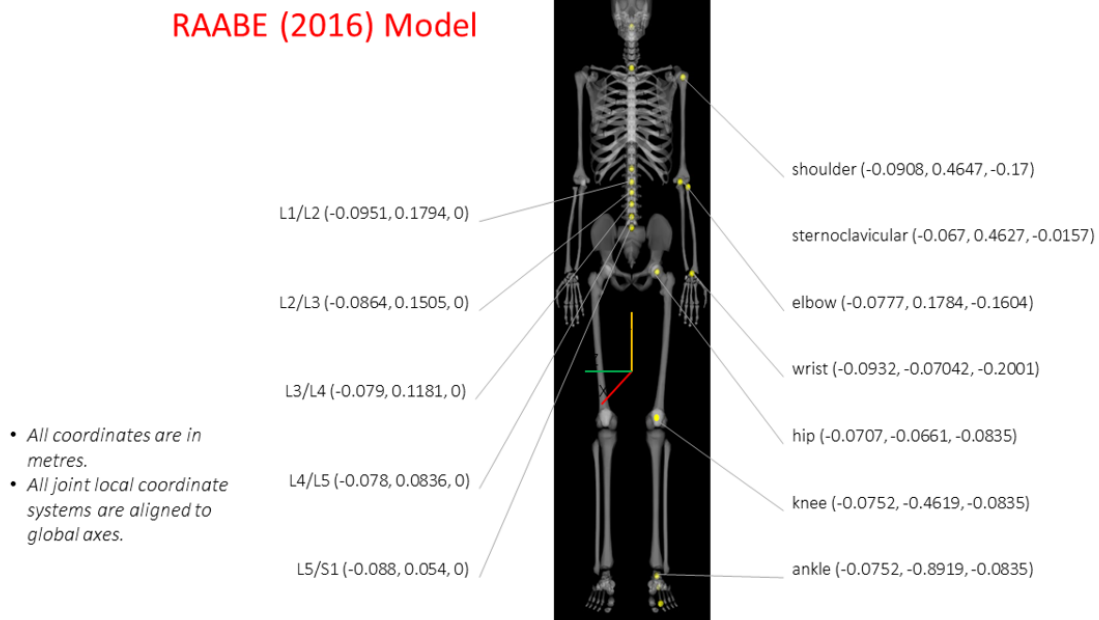


Figure 3. Two OpenSim skeleton-musculature models.

Considering the requirements of repositioning, we decided to integrate these two models and introduced additional joints to the spine locations at C0/C1 and T12/L1, as shown in Figure 4. The integrated model was then used as a template skeleton model for IAVCA. Note that the joints marked in red in Figure 4 are undefined and located by estimation using the ULB model as a basis. Therefore, additional efforts will be made in the future to refine and complete this model.

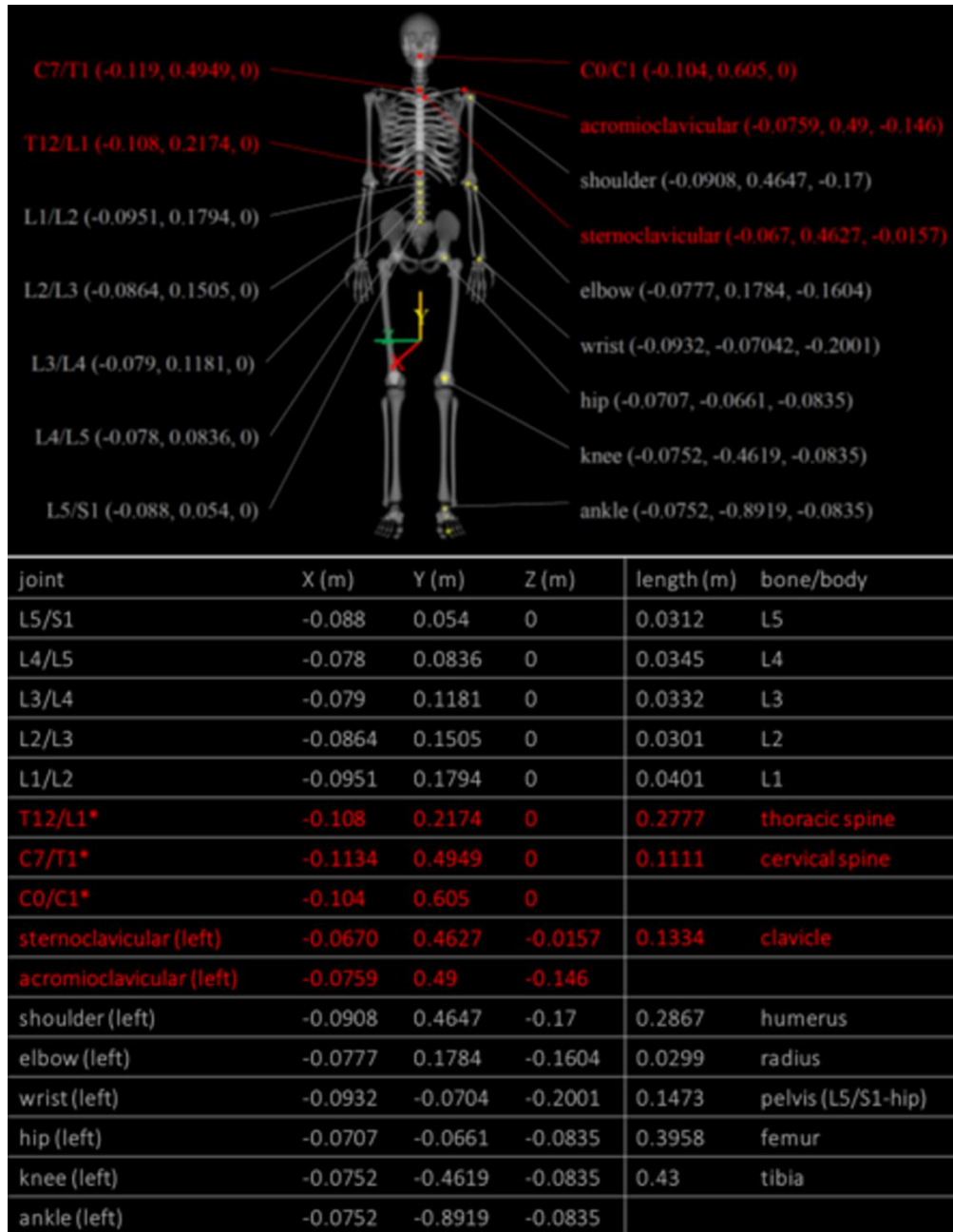


Figure 4. An integrated model being used as the template skeleton for IAVCA models.

Scaling

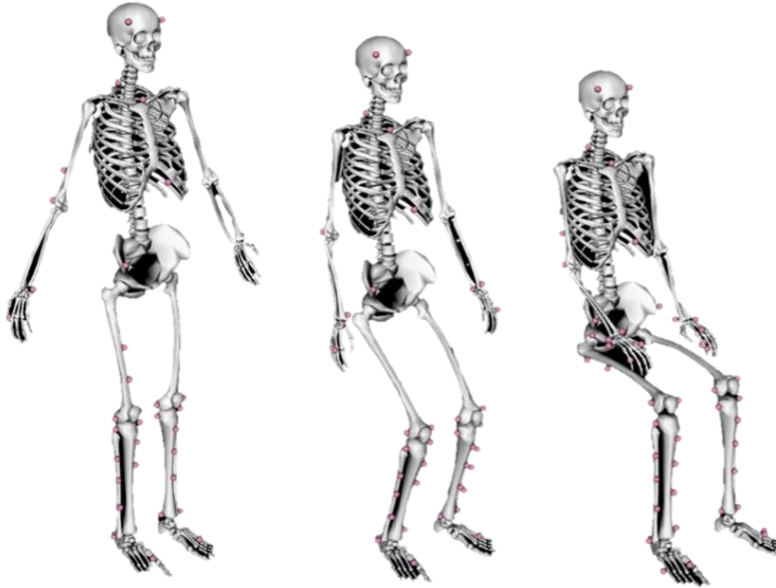
Humans differ in body size and shape and have varying sized skeleton. Thus, the template skeleton needs to be scaled to fit in to each individual IAVCA model. In OpenSim, the skeleton scaling can be accomplished if the landmark coordinates from a static pose are available. If landmark coordinates are not available, joint center nodes (i.e. the nodes corresponding to the respective joint centers in the template skeleton) can be identified from the bone structure of an IAVCA model. The bone lengths of the model skeleton can then be calculated using its joint center nodes, and the scale factor can be determined as the ratio between the model skeleton bone length and the template skeleton bone length.

Following this calculation, the template skeleton model was scaled within OpenSim for an individual IAVCA model using the scaling factor and the model subject weight as scaling parameters. This created the skeleton of each IAVCA model. Since IAVCA models used in this study have node-to-node correspondence, every model has the same set of joint center nodes. This greatly simplifies the scaling of the template skeleton to fit into an individual IAVCA model.

Posing and motion

The repositioning of a skeleton model from its initial pose to a different desired pose can be performed in OpenSim by interactively adjusting one or more joint angles. Motion may involve both simultaneous and sequential individual joint movements. The motion of an avatar can be represented by using OpenSim's forward kinematics software. The skeleton model is animated by initially identifying, from motion capture data, manual command or computation, the sequence of coordinate set changes composing the repositioning of the figure. Then, the animation cine frames can be generated from that sequence. The range of motion (i.e. joint angle limits) can be defined for each joint so that the created poses or motion appears natural, realistic and with biofidelity. Figure 5 illustrates the repositioning process of a model skeleton from standing to the seated position and from standing to squatting, respectively.

(A) From standing to seated position



(B) From standing to squatting



Figure 5. Posing with OpenSim skeleton model

Pose mapping

Following the posing of the figure, the skeleton pose information was converted from the OpenSim parametrization into IAVCA FE vertices repositioning. Skeleton pose information is described by a number of parameters: (a) joint angles, including

flexion/extension, adduction/abduction and rotation; and (b) joint center locations plus (c) the twist angle about the primary axis from the parent segment to the child segment. While the sequence of rotations is irrelevant in OpenSim due to the constraints used by the OpenSim model, it is important in FE repositioning. Therefore, we used the joint center locations plus the twist angle about the primary axis to define the pose and transfer this set of parameters from OpenSim to our FE morphing software.

Repositioning methodology development

Figure 6 shows the overall scheme to rapidly reposition IAVCA models as described in the previous sections. First, the model was re-segmented, during which the skeleton and soft tissues are grouped into different subsets. Then, the avatar joint centers that correspond to the joint locations of the OpenSim skeleton model were determined. This allows joint motion to be described in terms of the skeleton templated and applied correspondingly to the avatar. For a given joint motion (i.e. rotation and/or translation), we find the segments associated with the joint and calculate the change in position of the skeleton parts. Next, the skin and soft tissues around the joint were morphed, by a combination of skinning and morphing methods, so that the skeleton geometry was kept intact and the soft tissue geometry was changed smoothly according to the joint motion.

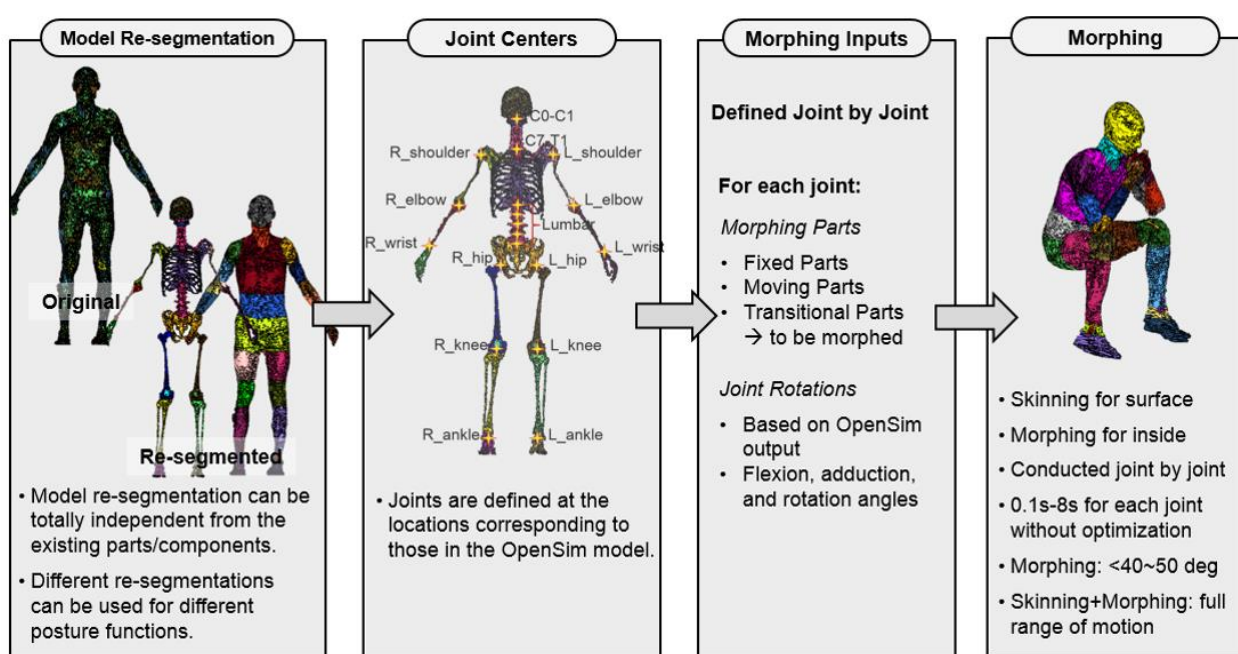


Figure 6. Framework for IAVCA model repositioning.

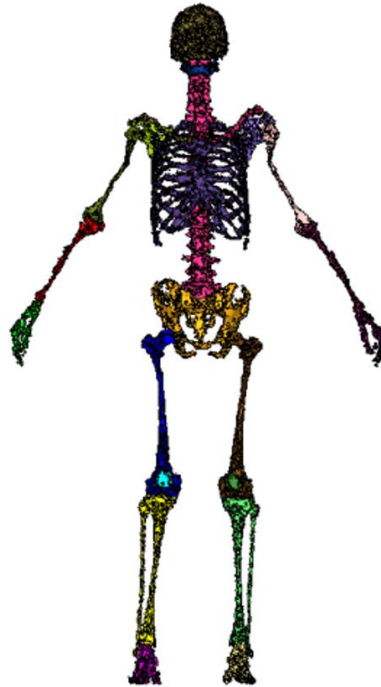
Re-Segmentation

The purpose of re-segmentation of the original IAVCA model (baseline model) is to separate the rigid (skeleton) anatomy from the deformable (soft tissues) anatomy in the human body and to define regions that will be morphed in the model repositioning process. Re-segmentation into various FE subsets will occur depending on the specific nature of the morphing needed in the regions where repositioning is computed (i.e. knees and/or elbows). Therefore, depending on the focused region of repositioning, re-segmentations into different FE subsets can be used for different repositioning functions. This is only an internal software secondary labeling, as the original anatomy labeling remains intact. A similar relabeling of superficial anatomy was performed in Zientara and Hoyt (1) to label appendages. Similarly, this process will only affect the assignments of elements to respective subsets and will not affect the geometry, nodal coordinates or element connections of the original model.

In this study, the IAVCA model re-segmentation was conducted using Hypermesh (31), a widely used FE pre-processor. To do this, the IAVCA models were first transformed into LS-DYNA Keyword format to facilitate the input and output, and then all the re-segmentations were based on the Keyword (.k) format. It should be noted that different input and output formats and an alternate choice of FE pre-processors may be chosen and applied for the sample purpose. The Keyword format was only chosen as an example. The original IAVCA model consists of 76 anatomy labeled FE sets, which are chosen to describe anatomy information rather than joint motion regions. To conduct some demonstrations for repositioning the models into different poses, we re-segmented the models into 53 new parts, as shown in Figure 7. Based on the common data structure shared among all IAVCA models in this study, re-segmentation can be automatically applied to all models, as shown in Figure 8.

(A) Bone re-segmentation

'Intervertebral_disc'
'Mandible'
'Skull'
'Teeth'
'Vertebrae'
'Clavicle_L'
'Scapula_L'
'Ribs'
'Humerus_L'
'Radius_Ulna_L'
'Hand_bones_L'
'Pelvis'
'Femur_L'
'Tibia_Fibula_L'
'Patella_L'
'Foot_bones_L'
'Clavicle_R'
'Scapula_R'
'Humerus_R'
'Radius_Ulna_R'
'Hand_bones_R'
'Femur_R'
'Tibia_Fibula_R'
'Patella_R'
'Foot_bones_R'



(B) Soft tissue re-segmentation

'Head'
'Neck'
'Chest'
'Abdomen'
'UpperArm_L'
'LowerArm_L'
'Hand_L'
'UpperArm_R'
'LowerArm_R'
'Hand_R'
'UpperLeg_L'
'LowerLeg_L'
'Foot_L'
'UpperLeg_R'
'LowerLeg_R'
'Foot_R'
'Shoulder_L'
'Elbow_L'
'Wrist_L'
'Shoulder_R'
'Elbow_R'
'Wrist_R'
'Hip'
'Knee_L'
'Ankle_L'
'Knee_R'
'Ankle_R'



Figure 7. IAVCA body re-segmentation. To reposition a model into different poses, we re-segmented it into 53 new parts.

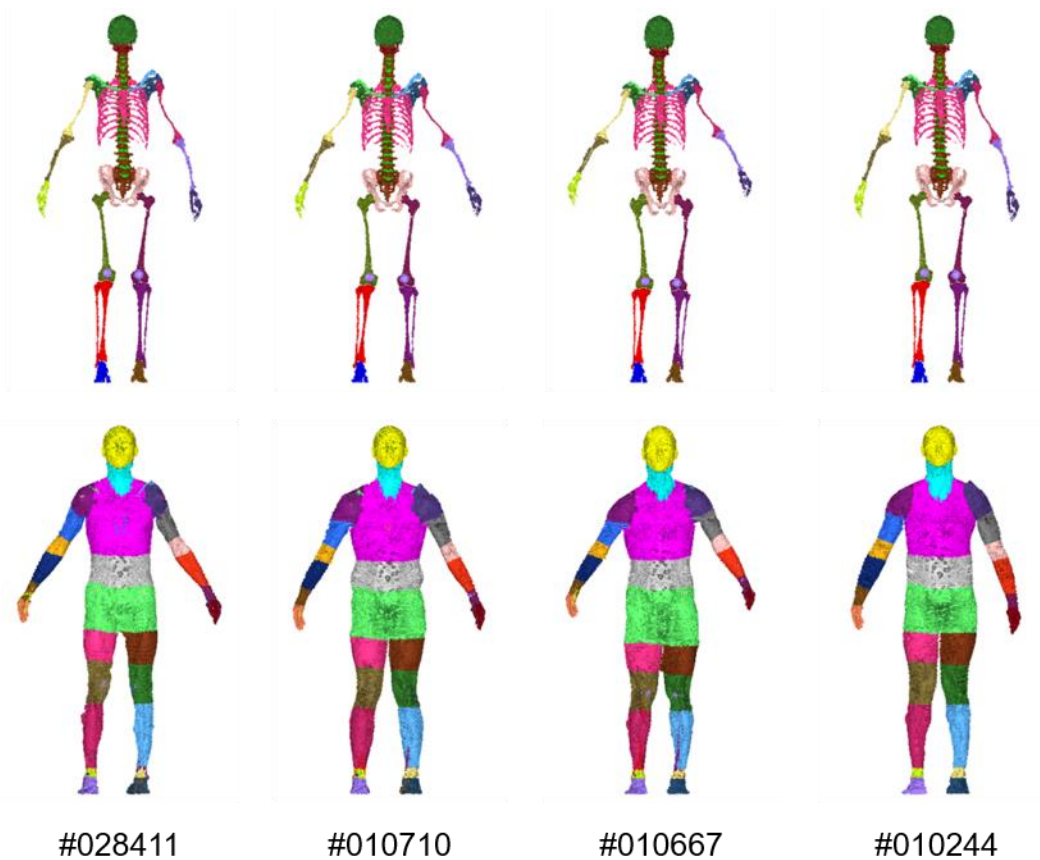


Figure 8. Re-segmentation automatically applied to all four IAVCA models. The colors represent labels of selected anatomy identified from re-segmentation.

Joint center determination

To reposition the IAVCA models, joint centers were identified based on the OpenSim joint definitions. This process was performed in HyperMesh by selecting nodes that corresponded to the joint centers defined by the template OpenSim skeleton model (Figure 4).

Mesh morphing

The mesh morphing method used in this study is based on the Radial Basis Functions (RBFs), which have been used extensively in the past to morph a baseline human FE model to any target geometries (38, 39). To perform the mesh morphing, corresponding landmarks need to be identified on both the target geometry model and the baseline human FE model, so that nodal displacement at each landmark location can be calculated. Using RBFs, a 3D displacement field throughout the entire space of the human geometry is calculated based on the landmark displacements. By applying this

displacement field to the baseline FE mesh, a new model with new geometry can be achieved. The basic formulas of the RBFs are provided below.

In general, the RBF takes the form in Eq. 1.

$$s(x) = p(x) + \sum_{i=1}^n \lambda_i \varphi (\|x - x_i\|) \quad (\text{Eq. 1})$$

where $p(x)$ is a low order polynomial, λ_i is the weighting coefficient, φ is the basis function, and $\|x - x_i\|$ is the Euclidean distance between x and x_i . In this study, because of the 3D coordinates of the nodes, the Euclidean distance between two nodes is shown below.

$$r_{ij} = \sqrt{(x_i - x_j)^2 + (y_i - y_j)^2 + (z_i - z_j)^2}$$

The first order polynomial is selected for $p(x)$ and the thin-plate spline function $\varphi(r) = r^2 \log r$ is selected as the basis function because it generally results in a smooth mesh.

Assume that the numbers of landmarks on the baseline model and correspondingly on the target geometry are both n . To compute the weight coefficient λ_i and the coefficients of the polynomial function $p(x)$, the RBF must be written in the matrix form (Eq. 2) by applying the interpolation requirements and boundary conditions:

$$\begin{pmatrix} A + \alpha I & B \\ B^T & 0 \end{pmatrix} \begin{pmatrix} \lambda \\ c \end{pmatrix} = \begin{pmatrix} T \\ 0 \end{pmatrix} \quad (\text{Eq. 2})$$

where A is an $n \times n$ matrix in which $A_{ij} = \varphi(r_{ij}) = r_{ij}^2 \log(r_{ij})$; α is a smoothing factor, with $\alpha = 0$ representing interpolation lacking smoothing, as is the case in this study; c is an unknown scalar;

$$B = \begin{bmatrix} 1 & x_1 & y_1 & z_1 \\ \vdots & \vdots & \vdots & \vdots \\ 1 & x_n & y_n & z_n \end{bmatrix}_{nx4}$$

where x , y , and z are the coordinates of the baseline landmarks; and

$$T = \begin{bmatrix} X_1 & Y_1 & Z_1 \\ \vdots & \vdots & \vdots \\ X_n & Y_n & Z_n \end{bmatrix}_{nx3}$$

where X , Y , and Z are the coordinates of the target.

Solving Eq. 2 can determine λ and c . Once λ and c are determined, by assuming the total number of nodes in the baseline model is N , the coordinates of the nodes in morphed model (T') can be calculated as shown in Eq. 3.

$$\begin{pmatrix} T' \\ 0 \end{pmatrix} = \begin{pmatrix} A' + \alpha I & B' \\ B'^T & 0 \end{pmatrix} \begin{pmatrix} \lambda \\ c \end{pmatrix} \quad (\text{Eq. 3})$$

where A' is an $N \times n$ matrix, in which $A_{ij} = \varphi(r_{ij}) = r_{ij}^2 \log(r_{ij})$, i is the number of nodes in the baseline model and j is the number of baseline landmarks; $\alpha = 0$ is used again assuming we aim to represent an exact interpolation;

$$T' = \begin{bmatrix} X_1 & Y_1 & Z_1 \\ \vdots & \vdots & \vdots \\ X_N & Y_N & Z_N \end{bmatrix}_{N \times 3}$$

where X , Y and Z are the coordinates of the nodes in the morphed model; and

$$B' = \begin{bmatrix} 1 & x_1 & y_1 & z_1 \\ \vdots & \vdots & \vdots & \vdots \\ 1 & x_N & y_N & z_N \end{bmatrix}_{N \times 4}$$

where x , y , and z are the coordinates of the nodes in the baseline model.

Skinning and morphing

Based on the results from examples of model repositioning, we observed that the RBF-based mesh morphing method was unable to provide realistically appearing body surface geometry if the joint rotation exceeded 50 degrees. Therefore, we adopted a hybrid algorithm by combining the Linear Blend Skinning (LBS) method and the RBF mesh morphing method in order to smoothly transform the mesh around the repositioned joint(s) to another pose.

LBS is the most commonly used algorithm to deform a mesh using skeletal structures (40). The main advantage of LBS is that it is not computationally intensive and still provides acceptable deformations in a large range of joint rotations. However, LBS typically only works for the skin surface mesh and is not designed to smoothly transform 3D solid meshes around the rigid skeletal structures.

To overcome this limitation, we performed the mesh transformation in two steps. First, LBS was used to transform the skin around the joint. Second, RBF was used to morph the 3D soft tissue meshes around the joint based on the transformed skin and skeletal meshes. By combining the skinning and mesh morphing methods, we resolved the problems associated with both mesh morphing (i.e. limited joint angle) and skinning (i.e. unable to accommodate solid tissues around the skeletal structures).

To accomplish the hybrid approach to morphing, the deformed skin surface was first modeled. The LBS method was used to compute the deformed node/vertex positions v'_i according to Eq. 4.

$$v'_i = (\sum_{j=1}^m w_{i,j} T_j) v_i \quad (\text{Eq. 4})$$

where v_i is the i -th node original position, T_j is the spatial transformation based on the motion of bone j , m is the total number of bones and $w_{i,j}$ describes the amount of influence

of bone j on node i . A common requirement is that $w_{i,j} \geq 0$ and $w_{i,1} + \dots + w_{i,m} = 1$ (partition of unity). In this study, for each joint motion, only two bones were involved ($m = 2$) and we assigned the weighting factor $w_{i,j}$ to represent the normalized ratio between the distances to the upper and lower bounds of the transitional area.

The effectiveness and robustness of this method is shown by the simplified example illustrated in Figure 9. The example consisting of two bones (stationary and moving) and three soft tissue regions (stationary, transitional and moving) was designed to test the mesh equality of the deformed region. We judged mesh quality qualitatively in terms of the apparent realistic appearance of the elements in the deformed region. Figure 9 shows cases of the resultant deformed region after using the RBF morphing approach, the LBS skinning approach and then the combined skinning and morphing methods, respectively.

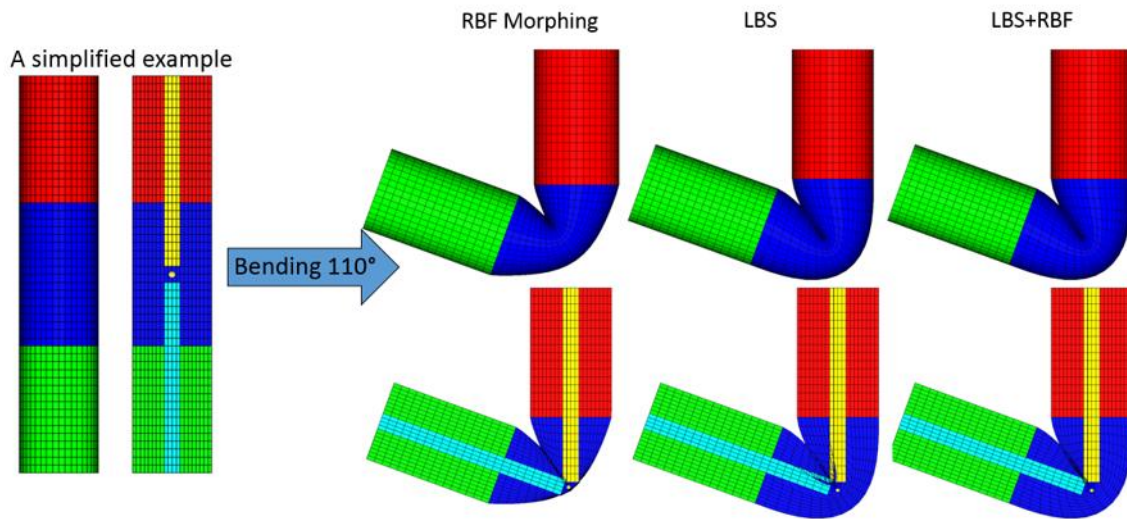


Figure 9. A simplified example to demonstrate the robustness of the combined linear blend skinning and radial basis function (LBS+RBF) repositioning method. Blue transitional elements represent those undergoing affine transformations to bend the joint. Red elements are stationary and green elements are those that undergo translation. Yellow and light blue represent two bone segments on either side of the joint. The bending results are shown with (bottom) and without (top) the bone segments.

The results of a 110° bending of the joint are shown on the right of Figure 9. With a 110° rotation angle, the mesh results by the RBF mesh morphing method alone were not physically realistic and many elements were squeezed around the outer surface of the joint. In contrast, the LBS method alone generated a better surface geometry. However, the resulting 3D soft tissue mesh was overlapped with the rigid bone mesh, which is not acceptable. By coming the skinning and mesh morphing method (LBS+RBF),

the surface geometry was determined by the skinning method, whereas the 3D soft tissue elements were morphed by RBF. As a result, both the outside and the inside of the transitional elements were mesh with good quality.

Software system development

A software system was developed that implements the approach described above and provides the basic capabilities for the repositioning of IAVCA models. Its schematic is shown in Figure 10. The current version of the system is built using the MATLAB® platform.

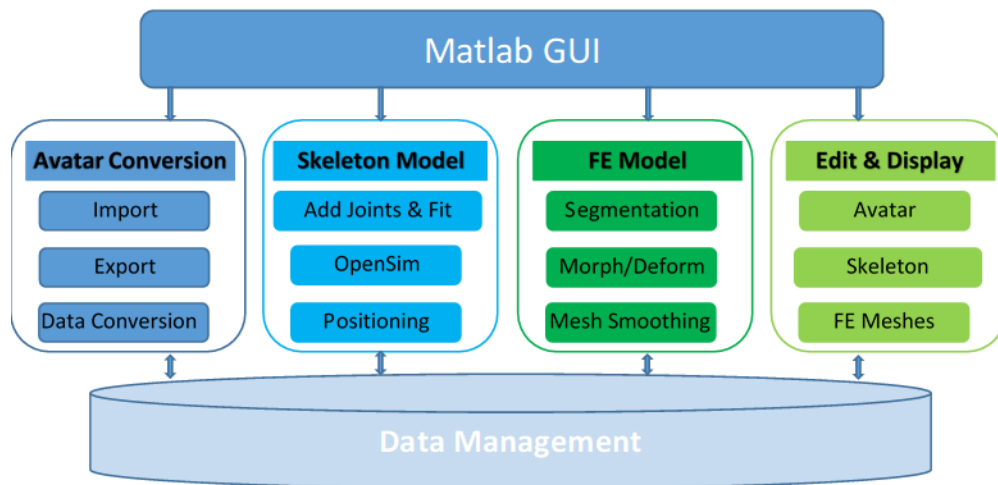
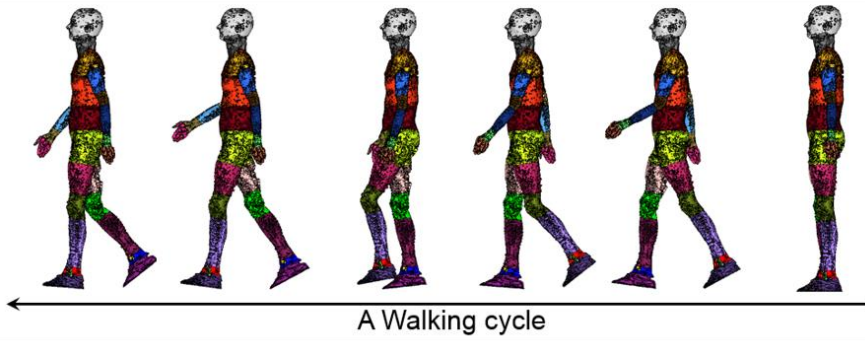


Figure 10. Overall architecture of software system

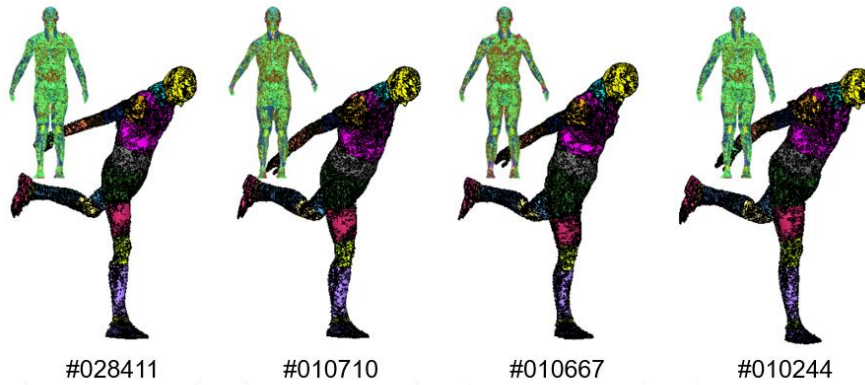
RESULTS

To test the effectiveness of our hybrid repositioning approach and the associated software system, four IAVCA models were repositioned in four cases: (1) from standing to walking; (2) from standing to running; (3) from standing to sitting; and (4) from standing to squatting. The results of these cases are shown in Figure 11. While joint angle changes were moderate for cases (1) and (2), large rotations of joints occurred in cases (3) and (4). Figure 11 shows that even for cases (3) and (4), the combined skinning and morphing method was still able to create natural and realistic mesh deformations for the regions around the joints with large rotations.

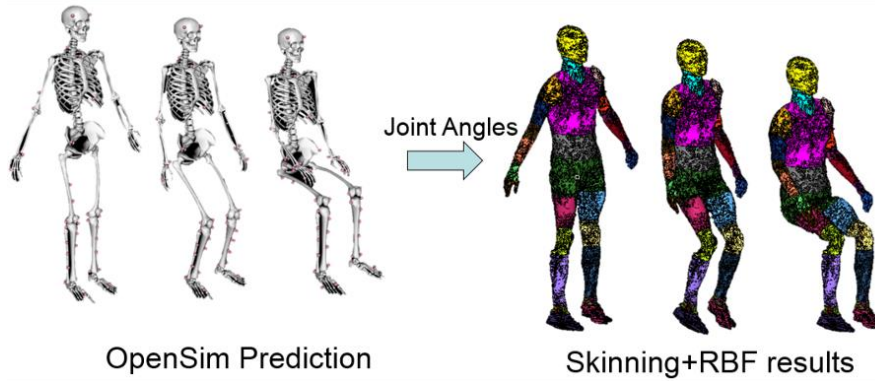
(A) From standing to walking



(B) From standing to running



(C) From standing to sitting



(D) From standing to squatting

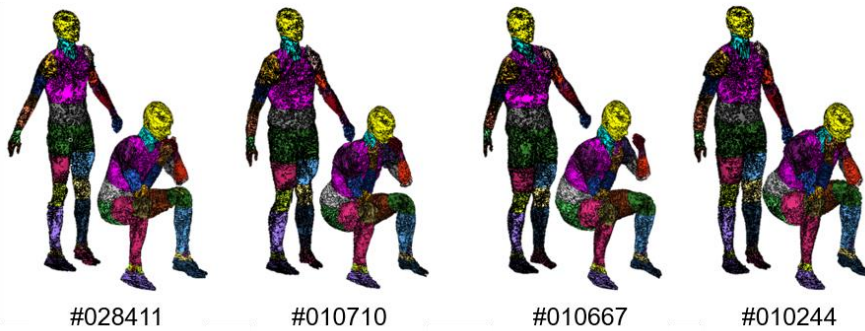


Figure 11. Results of case studies.

The case studies also indicate that it is crucial to have a high biofidelity skeletal model, since human body poses and motions require the set of human joints to manipulate the figure to simulate a realistic model. The skeleton model we integrated and used in this study has sufficient joints and degrees-of-freedom (DoFs) needed to show various body poses and motions. These include neck and head rotation and bending, arm rotation and bending at the shoulder, elbow rotation and bending, leg rotation and bending at the pelvis, rotation at the pelvis, knee bending, and cervical and lumbar vertebrae bending. In OpenSim, the IAVCA model skeleton (scaled skeleton) can be repositioned from its initial pose to the desired pose by interactively adjusting its joint angles. The dynamic motion of the skeleton can be created in OpenSim via either forward kinematics or animation with motion capture data. Realistic poses and motions with high biofidelity can be created by choice of appropriate transformations for the joints and muscles of the skeleton while applying realistic constraints on the kinematics and range of joint motions. As shown in Figure 11, only a few transformations were necessary to create the squatting figure from the standing position.

DISCUSSION

IAVCA models have many opportunities for use in future applications. While they are approximate representations of a human, IAVCA model anatomy provides individualized anatomical information similar to that which may be acquired from medical imaging, specific to the spatial resolution of the avatars. Further modifications to the avatars' composition, based on acquired medical scan information, can increase the medical fidelity of this anatomical information.

Past development and research of singular or a small number of unique human models have illustrated applications in various fields of study in which avatars can be valuable. Several projects, including THUMS and GBHMC, produced models mainly to computerize the study of repeated simulations of dangerous or potentially fatal automobile accidents. The SANTOS avatar (Univ. of Iowa) (41) was developed primarily for military simulation purposes. The Zygote human model (Zygote Media Group, Inc.) was created to provide a 3D CAD model for medical device designers. The National Institute of Information and Communications Technology (NICT) of Japan and the IT'IS Foundation (Zurich, Switzerland) developed models to employ in radio wave and microwave dosimetry studies (42).

The common factor among the applications listed previously is that the computer human models allow for testing, especially repeated testing, under conditions that could be harmful or fatal to a human and/or expensive for physical testing with a manikin. IAVCA can act as a substitute within simulations and testing in order to forgo the risks inherent in human subjects involvement where danger exists, to eliminate ethics issues with the use of human subjects and to reduce the expenses, logistics and time spent working with human subjects. IAVCA can be used as safe alternatives in applications that need specific individuals, including participation in different experiences or circumstances with varying environmental conditions, and interact with other avatars, structures and objects. When

integrated with other software, IAVCA would be able to simulate individual human response to forces, electro-magnetic radiation, heat, cold and other stimuli. Also, they can be included in virtual/augmented reality applications to provide more realistic experiences than when generic avatars are employed.

CONCLUSIONS

The individualized avatar with complete anatomy has opened up a wide range of potential applications for avatars that have the anatomical composition and appearance of real individuals. In order to reposition an IAVCA model from its initial standing pose to any desired pose and to create a sequence of such poses to simulate motion, we developed a systematic approach with three steps: (1) IAVCA data structure conversion from vertex-tetrahedron data to Keyword format; (2) Skeleton model construction and simulation; and (3) IAVCA model re-segmentation and mesh morphing to create realistic shapes of superficial anatomy after repositioning. By using an integrated skeleton model in OpenSim, we were able to create natural, realistic and biofidelic poses and motions for IAVCA models. By combining RBF-based mesh morphing with LBS, we developed an innovative and effective method for treating excessive soft tissue deformations due to large joint motion. Through case studies where four IAVCA models were repositioned to four new poses, we tested the repositioning approach and the associated software system and proved its effectiveness and usefulness.

REFERENCES

1. Zientara GP, Hoyt RW. Individualised avatars with complete anatomy constructed from the ANSUR II 3-D anthropometric database. *Int J Digital Human.* 2016;1(4):389-411.
2. Vezin P, Verriest JP, editors. Development of a set of numerical human models for safety. 19th International Technical Conference on the Enhanced Safety of Vehicles (ESV); June 2005; Washington, D. C.
3. Jani D, Chawla A, Mukherjee S, Goyal R, Nataraju V. Repositioning the human body lower extremity FE model. *SAE Int J Passeng Cars – Mech Syst.* 2009;2(1):1024-30.
4. Jani D, Chawla A, Mukherjee S, Goyal R, Vusirikala N, editors. Human body FE model repositioning: a step towards posture specific - human body models (PS-HBM). IRCOBI Conference; September 2009; York, United Kingdom.
5. Fedorov A, Beichel R, Kalpathy-Cramer J, Finet J, Fillion-Robin J-C, Pujol S, et al. 3D Slicer as an image computing platform for the Quantitative Imaging Network. *Magn Reson Imaging.* 2012;30(9):1323-41.
6. Kikinis R, Pieper SD, Vosburgh KG. 3D Slicer: A Platform for Subject-Specific Image Analysis, Visualization, and Clinical Support. In: Jolesz FA, editor. *Intraoperative Imaging and Image-Guided Therapy.* New York, NY: Springer New York; 2014. p. 277-89.
7. Yushkevich PA, Piven J, Hazlett HC, Smith RG, Gee JC, Gerg G. User-guided 3D active contour segmentation of anatomical structures: Significantly improved efficiency and reliability. *Neuroimage.* 2006;31(3):1116-28.
8. Christ A, Kainz W, Hahn EG, Honegger K, Zefferer M, Neufeld E, et al. The virtual family – development of surface-based anatomical models of two adults and two children for dosimetric simulations. *Phys Med Biol.* 2010;55(2):N23-N38.
9. Gosselin M-C, Neufeld E, Moser H, Huber E, Farcito S, Gerber L, et al. Development of a new generation of high-resolution anatomical models for medical device evaluation: the virtual population 3.0. *Phys Med Biol.* 2014;59(18):5287-303.
10. The Virtual Population. Development of a new generation of high-resolution anatomical models for medical device evaluation. In: SPEAG AG, editor. *EuCAP 2016.* Davos, Switzerland, 2016. p. 2.
11. Sim4Life [Internet]. Zurich, Switzerland: Zurich MedTech AG. 2019. Available from: <https://zmt.swiss/sim4life/>.
12. Cherubini E, Chavannes N, Kuster N, editors. Realistic skeleton based deformation of high-resolution anatomical human models for electromagnetic simulations. Abstracts of the 30th Annual Meeting of the Bioelectromagnetics Society; June 2008; San Diego, CA.
13. Community BO. Blender - a 3D modelling and rendering package. Amsterdam: Stichting Blender Foundation; 2018.
14. COMSOL Multiphysics®. v 5.4 ed. Stockholm, Sweden: COMSOL AB.
15. Maya [Internet]. San Rafael, CA: Autodesk, Inc. 2019. Available from: <https://www.autodesk.com/products/maya/overview>.
16. Delp SL, Anderson FC, Arnold AS, Loan P, Habib A, John CT, et al. OpenSim: open-source software to create and analyze dynamic simulations of movement. *IEEE Trans Biomed Eng.* 2007;54(11):1940-50.

17. Anybody Modeling System [Internet]. Aalborg, Denmark: Anybody Technology. 2017. Available from: <https://www.anybodytech.com/>.
18. Maeno T, Hasegawa J, editors. Development of a finite element model of the total human model for safety (THUMS) and application to car-pedestrian impacts. Proceedings of 17th International ESV Conference 2001.
19. PIPER Software [Internet]2017. Available from: <http://piper-project.org/>.
20. Bender [Internet]. Clifton Park, NY: Kitware, Inc. 2014. Available from: <https://public.kitware.com/Wiki/Bender>.
21. Anguelov D, Srinivasan P, Koller D, Thrun S, Rodgers J, Davis J. SCAPE: Shape Completion and Animation of People. ACM Trans Graph. 2005;24(3):408-16.
22. Reed M, P., Raschke U, Tirumali R, Parkinson MB, editors. Developing and implementing parametric human body shape models in ergonomics software. 3rd International Digital Human Modeling Conference; 2014; Tokyo, Japan.
23. Park B-K, Lumeng JC, Lumen CN, Ebert SM, Reed MP. Child body shape measurement using depth cameras and a statistical body shape model. Ergonomics. 2015;58(2):301-9.
24. Park B-KD, Reed MP, Kaciroti N, Love M, Miller AL, Appugliese DP, et al. ShapeCoder: A new method for visual quantification of body mass index in young children. *Pediatr Obes*. 2016;13(2):88-93.
25. Park B-K, Reed MP. Parametric body shape model of standing children aged 3-11 years. *Ergonomics*. 2015;58(10):1714-25.
26. Park B-KD, Ebert S, Reed MP. A parametric model of child body shape in seated postures. *Traffic Injury Prevention*. 2017;18(5):533-6.
27. Loper M, Mahmood N, Romero J, Pons-Moll G, Black MJ. SMPL: A Skinned Multi-Person Linear Model. ACM Trans Graph. 2015;34(6):248:1-:16.
28. Alliez P, Jamin C, Rineau L, Tayeb S, Tournois J, Yvinec M. 3D Mesh Generation. CGAL User and Reference Manual 48 [online]2016. p. <http://doc.cgal.org/4.8/Manual/packages.html#PkgSurfaceMesher3Summary>.
29. Fang Q, Boas D, editors. Tetrahedral mesh generation from volumetric binary and gray-scale images. Proceedings of IEEE International Symposium on Biomedical Imaging 2009; 2009.
30. LS-PrePost [Internet]. Livermore, California: Livermore Software Technology Corporation. 2015. Available from: <https://www.lstc.com/products/ls-prepost>.
31. HyperMesh [Internet]. Troy, MI: Altair Engineering. 2017. Available from: <https://www.altair.com/hypermesh/>.
32. Seth A, Hicks JL, Uchida TK, Habib A, Dembia CL, Dunne JJ, et al. OpenSim: Simulating musculoskeletal dynamics and neuromuscular control to study human and animal movement. *PLoS Comput Biol*. 2018;14(7):e1006223.
33. Holzbaur KR, Murray WM, Delp SL. A model of the upper extremity for simulating musculoskeletal surgery and analyzing neuromuscular control. *Ann Biomed Eng*. 2005;33(6):829-40.
34. Raabe ME, Chaudhari AMW. An investigation of jogging biomechanics using the full-body lumbar spine model: model development and validation. *J Biomech*. 2016;49(7):1238-43.
35. Arnold EM, Ward SR, Lieber RL, Delp SL. A Model of the Lower Limb for Analysis of Human Movement. *Ann Biomed Eng*. 2010;38(2):269-79.

36. Hamner SR, Seth A, Delp MD. Muscle contributions to propulsion and support during running. *J Biomech.* 2010;43(14):2709-16.
37. Christophy M, Senan NAF, Lotz JC, M. ORO. A musculoskeletal model for the lumbar spine. *Biomech Model Mechanobiol.* 2012;11:19-34.
38. Hu J, Fanta A, Neal MO, Reed MP, Wang J-T, editors. Vehicle crash simulations with morphed GHBM human models of different stature, BMI and age. 4th International Digital Human Modeling Conference (DHM2016); 2016; Montreal, Quebec, Canada.
39. Zhang K, Cao L, Fanta A, Reed MP, Neal MO, Wang M, et al. An automated method to morph finite element whole-body human models with a wide range of stature and body shape for both men and women. *J Biomech.* 2017;60:253-60.
40. Kavan L. Part I: Direct Skinning Methods and Deformation Primitives. 2014. p. <https://skinning.org/direct-methods.pdf>.
41. Abdel-Malek K, Arora J, Frey Law L, Swan C, Beck S, Xia T, et al., editors. SANTOS: A Digital Human in the Making. IASTED International Conference on Applied Simulation and Modeling; June 2008; Corfu, Greece.
42. Makarov SN, Noetscher GM, Yanamadala J, Piazza MW, Louie S, Prokop A, et al. Virtual Human Models for Electromagnetic Studies and Their Applications. *IEEE Rev Biomed Eng.* 2017;10:95-121.